Diversity of strains in the Pseudomonas syringae complex causing bacterial stem blight of Alfalfa (Medicago sativa) in the United States

Savana M. Lipps, Claudia Castell-Miller, Cindy E. Morris, Satoshi Ishii, Deborah A. Samac

HAL Id: hal-04573014
https://hal.inrae.fr/hal-04573014

Submitted on 13 May 2024

Population Biology

Diversity of Strains in the *Pseudomonas syringae* Complex Causing Bacterial Stem Blight of Alfalfa (*Medicago sativa*) in the United States

Savana M. Lipps,[1] Claudia Castell-Miller,[1] Cindy E. Morris,[2] Satoshi Ishii,[3,4] and Deborah A. Samac[1,5,†]

[1] Department of Plant Pathology, University of Minnesota, St. Paul, MN 55108, U.S.A.
[2] INRAE, Pathologie Végétale, F-84140, Montfavet, France
[3] Department of Soil, Water, and Climate, University of Minnesota, St. Paul, MN 55108, U.S.A.
[4] BioTechnology Institute, University of Minnesota, St. Paul, MN 55108, U.S.A.
[5] U.S. Department of Agriculture-Agricultural Research Service-Plant Science Research Unit, St. Paul, MN 55108, U.S.A.

Abstract

Alfalfa growers in the Intermountain West of the United States have recently seen an increased incidence in bacterial stem blight (BSB), which can result in significant herbage yield losses from the first harvest. BSB has been attributed to *Pseudomonas syringae* pv. *syringae* and *P. viridiflava*; however, little is known about the genetic diversity and pathogenicity of these bacteria or their interaction with alfalfa plants. Here, we present a comprehensive phylogenetic and phenotypic analysis of *P. syringae* and *P. viridiflava* strains causing BSB on alfalfa. A multilocus sequence analysis found that they grouped exclusively with *P. syringae* PG2b and *P. viridiflava* PG7a. Alfalfa symptoms caused by both bacterial groups were indistinguishable, although there was a large range in mean disease scores for individual strains. Overall, PG2b strains incited significantly greater disease scores than those caused by PG7a strains. Inoculated

plants showed browning in the xylem and collapse of epidermal and pith parenchyma cells. Inoculation with a mixture of PG2b and PG7a strains did not result in synergistic activity. The populations of PG2b and PG7a strains were genetically diverse within their clades and did not group by location or haplotype. The PG2b strains had genes for production of the phytotoxin coronatine, which is unusual in PG2b strains. The results indicate that both pathogens are well established on alfalfa across a wide geographic range and that a recent introduction or evolution of more aggressive strains as the basis for emergence of the disease is unlikely.

Keywords: bacteriology, multilocus sequence analysis (MLSA), pathogenicity, *Pseudomonas syringae*, *Pseudomonas viridiflava*

Bacterial stem blight (BSB) of alfalfa was first reported in the United States in 1904 in Colorado, where it caused significant yield losses in both young and older stands (Sackett 1910). Overall, yield losses of up to 50% from the first forage harvest have been reported. BSB has also been documented in Europe, Australia, and Iran (Ansari et al. 2019; Gray and Hollingsworth 2015). There were relatively few reports of BSB on alfalfa during the latter half of the 20th century, but this disease has recently emerged as a significant problem in the western and central United States. As of 2023, BSB has been found in California, Oregon, Utah, Colorado, Wyoming, Minnesota, and Ohio. BSB symptoms include necrotic lesions on stems, chlorosis and necrosis of leaves, and curling and deformation of the stem apex. Currently, there are no commercially available sources of resistance for this disease nor effective control measures except for premature harvest of the forage.

Initially, BSB was determined to be caused by strains of *Pseudomonas syringae* pv. *syringae* (Gray and Hollingsworth 2015).

The pathovar's taxonomic status was based originally on the original host of isolation; however, it has become ambiguous because it does not provide clarity on the phylogenetic position among a larger species complex. *P. viridiflava*, a species within the *P. syringae* complex, was isolated from alfalfa with BSB symptoms in California and Utah and was shown to also be a causal agent of the disease (Lipps et al. 2019).

The *P. syringae* species complex is an amalgam of closely related pseudomonads that altogether comprises nine genomospecies determined by DNA-DNA hybridization, at least 13 phylogroups determined by multilocus sequence analysis (MLSA), and 60 pathovars that cause similar symptoms including specks, spots, blights, and cankers on a wide range of host plants (Berge et al. 2014; Gardan et al. 1999; Lamichhane et al. 2015). Strains in phylogroup 2 (PG2) are the most ubiquitous bacteria of the complex, existing in a wide range of environments from agricultural to natural landscapes (Berge et al. 2014; Morris et al. 2008). In agriculture, PG2 strains have caused eight major outbreaks on annual plants since 2000, which make up 11% of all outbreaks caused by the *P. syringae* species complex worldwide since the start of the century (Lamichhane et al. 2015). In nature, *P. syringae* has the potential to influence cloud processes leading to rainfall, due to its activity as an ice nucleating particle, thereby having a role in the global water cycle (Morris et al. 2008). PG2 strains are typically more aggressive on agricultural plants than strains from other phylogroups, seeming to be able to readily make the switch from an epiphytic to an endophytic phase in the disease causation process (Xin et al. 2018). In a 2016 study of 216 strains across the *P. syringae* species complex, it was demonstrated that those from PG2 had the most consistent ice nucleation activity (INA) (Berge et al. 2014). Strains from this group also have an arsenal of virulence factors that contribute to success as a phytopathogen, including production of toxins such as coronatine,

syringomycin, syringopeptin, tabtoxin, and phaseolotoxin (Bricout et al. 2022), and a canonical tripartite pathogenicity island (T-PAI) that encodes the type III secretion system (T3SS) for delivery of effector molecules (Xin et al. 2018). *P. syringae* strains have been placed into a phylogenetic context via single-gene sequencing, MLSA and multilocus sequence typing, repetitive element sequence-based PCR (rep-PCR), and, more recently, whole-genome sequencing (Berge et al. 2014; Bull and Koike 2015; Dillon et al. 2019; Hwang et al. 2005).

P. viridiflava, comprising phylogroups 7a (PG7a) and 7b (Berge et al. 2014), has been shown to infect a range of monocot and dicot hosts (Lipps and Samac 2022) and since 2000 has been responsible for at least 13 outbreaks of diseases on annual plants comprising 18% of all outbreaks caused by the *P. syringae* species complex (Lamichhane et al. 2015). In addition, this species exists as an endophyte, epiphyte, and saprophyte in both agricultural and natural environments (Bartoli et al. 2014; Bordjiba and Prunier 1991; Samad et al. 2017). Differentiating characteristics of the PG7 phylogroup include pectate lyase as a virulence factor, colony type (mucoid or non-mucoid), antibiotic resistance, and atypical pathogenicity islands (single-partite pathogenicity island [S-PAI] in PG7a or tripartite pathogenicity island [T-PAI] in PG7b) (Bartoli et al. 2015). Delineation of *P. viridiflava* from other members within the *P. syringae* species complex has been a major research focus in the past decade (Baltrus et al. 2017; Berge et al. 2014; Bull and Koike 2015; Dillon et al. 2019). Genetic relationships have been investigated through DNA-DNA hybridization, comparisons of 16S rRNA and housekeeping gene sequences, molecular fingerprinting, and comparisons of whole-genome sequences (Anzai et al. 2000; Berge et al. 2014; Dillon et al. 2019; Gardan et al. 1999).

There have been several reports of *P. viridiflava* causing disease in synergy with other plant-pathogenic bacteria. For example, *P. viridiflava* causes tomato pith necrosis alone and in association with seven other *Pseudomonas* species. The latter leads to greater disease severity (Lamichhane and Venturi 2015). Additionally, bacterial strains across different species, including *Pectobacterium carotovorum*, *Pseudomonas marginalis*, *P. fluorescens*, and *P. viridiflava*, have been reported to cause broccoli head rot, of which symptoms were ultimately attributed to this bacterial complex (Canaday et al. 1991). In alfalfa, several endoparasitic nematodes may act synergistically with *P. viridiflava* to contribute to the root rot complex (Bookbinder et al. 1982). Potential synergy of PG2b and PG7a strains in causing BSB has not been explored previously.

There has not been a comprehensive analysis of BSB-causing bacteria that explores the phenotypic, phylogenetic, and genomic characteristics of these pathogens. To improve understanding of the genetic diversity and pathogenicity of the strains in the *P. syringae* complex causing BSB of alfalfa, we established a collection of strains from symptomatic alfalfa leaf and stem samples from California, Minnesota, Ohio, Oregon, and Utah. The strains were evaluated for pathogenicity and ice-nucleation activity and were used for MLSA. Genome sequences of a subset of PG2b and PG7a strains varying in virulence (Lipps et al. 2022) were compared to further explore genomic data relevant to pathogenicity. Analysis of the genetic and pathogenic diversity of the populations within the *P. syringae* complex causing BSB on alfalfa is critical to determine if contemporary disease outbreaks are due to a recent emergence of the pathogens, as well as to develop effective control practices, including disease-resistant cultivars.

This research addresses the overall question regarding the genetic scope of the causal agent(s) of BSB. This will inform what causal agents to target initially when surveying and diagnosing/screening for BSB in the future. In this study we characterize previously understudied populations of *Pseudomonas*, the BSB-causing strains, by: (i) defining their genetic diversity and phylogenetic placement in the *P. syringae* complex and (ii) assessing key phenotypic characteristics including pathogenicity and INA.

Materials and Methods

Bacterial isolation, identification, and storage

Stems from alfalfa plants were collected in 2016, 2017, 2019, and 2020 from eight locations in the western and central United States: in California from Scott Valley, Shasta Valley, Susanville, and Tulelake; in Oregon from Klamath Falls; in Utah from Cornish; in Minnesota from St. Paul; and in Ohio from South Charleston (Supplementary Table S1). A modified ice nucleation assay was used to identify alfalfa stems that likely harbored PG2 strains (Hirano et al. 1987). A stem from a sampled plant was processed to remove the lowest internode and all leaves. Then, the three lowest remaining internodes were placed into a 10-ml glass test tube containing 7 ml of sterile 10 mM potassium phosphate buffer, pH 7. Tubes were placed in a sonicating water bath at room temperature for 10 min, then transferred to a recirculating low-temperature incubator (Polyscience, Niles, IL). To identify samples that potentially contained *Pseudomonas*, the tubes were held at $-4.5°C$ for 10 min, and tubes with frozen buffer were stored at $-20°C$. Storage of bacteria with similar population sizes at $-20°C$ was previously shown to not affect viability (Hirano et al. 1994; D. A. Samac, *unpublished data*). For pathogen isolation, tubes were thawed at room temperature and sonicated for 10 min, and serial dilutions were cultured on King's B medium. Single colonies that fluoresced under UV light were selected randomly and streaked on new agar plates to obtain pure cultures. Single isolates were retained from a processed stem based on colony PCR as described below.

Colony PCR was used to identify *P. syringae* and *P. viridiflava* isolates using a multiplex PCR assay. Amplification of a 360-bp fragment from a putative lipoprotein and monooxygenase gene specific to *P. viridiflava* (Bartoli et al. 2014) and a 742-bp portion of the lipodepsinonapeptide toxin gene of *P. syringae* pv. *syringae* (Sorensen et al. 1998) were used to rapidly distinguish between the two pathogens (Lipps et al. 2019). All confirmed *P. syringae* and *P. viridiflava* isolates were stored at $-80°C$ in 20% glycerol. In this study, 94 PG2 and 29 PG7 strains were used for phenotypic and genetic characterization (Supplementary Table S2).

Pathogenicity testing

Alfalfa plants from the cultivar CUF101, susceptible to BSB, were grown to the three-leaf stage (about 3 weeks) in a growth chamber at $22°C$ with a 16-h light cycle. Stems were wounded at the second or third internode with a tuberculin needle, and then a bacterial suspension (optical density at 600 nm [OD_{600}] = 0.1; $\sim 1 \times 10^8$ CFU/ml) was applied with a sponge at the wound site. Six plant replicates were inoculated for each isolate. To test for combined pathogenicity/synergism of *P. syringae* and *P. viridiflava*, the bacterial suspension of each species was diluted to $OD_{600} = 0.05$ and then combined. Symptoms were rated 7 to 10 days postinoculation with a 1-to-5 scoring system. Symptoms on stems were rated 1 = no necrosis on stem, 2 = minimal browning at wound site, 3 = lesion extends from wound site less than 5 mm, 4 = lesion extends more than 5 mm from wound site, and 5 = lesion causes stem collapse/breakage. Symptoms on leaves were rated 1 = no symptoms on leaves, 2 = leaf symptoms limited to one node, 3 = yellowing on leaves on two or more nodes, 4 = yellowing of leaves systemic, 5 = leaf necrosis with defoliation. R version 4.0.2 was used for statistical analysis. The Pearson correlation coefficient was calculated for the relationship between leaf and stem scores using the function cor() in R. Student's *t* test was used (t.test function in R) with a significance level of 0.05 to identify significant differences in the mean stem and leaf scores induced by *P. syringae* PG2-grouping strains versus PG7-grouping strains. Analysis of variance (ANOVA) was conducted using R function lm() and ANOVA() with a significance level of 0.05.

INA

Each isolate was tested for INA. A bacterial suspension of each isolate ($OD_{600} = 0.1$ representing approximately 1×10^8 CFU/ml)

was prepared in 10 mM K_2PO_4 buffer, pH 7, and serial dilutions of 1:10, 1:100, 1:1,000, and 1:10,000 of the suspension were made. Three technical replicates of each dilution were used. Each dilution for individual isolates was kept on ice for 1 h to activate the ice nucleating properties of the bacteria. Tubes with 1 ml of each suspension were submerged in a $-4.5°C$ bath for 10 min, and the dilution and number of replicates at which the isolate froze were recorded. Isolates that froze on average at 1×10^6 CFU/ml (the 1:1,000 dilution) or lower were considered ice nucleation active (Bartoli et al. 2014).

Microscopy

Plants were inoculated with *P. syringae* PG2 strain SV921, *P. viridiflava* PG7 strain Tule157, and mock inoculated with water using the inoculation method previously described. At 7 days postinoculation, a microtome was used to make cross sections at and above the inoculation site. Cross sections were ~100-μm thick, and sections were taken up to 0.75 cm above the point of inoculation. Cross sections were placed on slides and imaged with a Nikon Eclipse NI-U Light Microscope. The DS-Ri1 Digital Color was used to obtain images. NIS-Elements (AR version) software was used for image acquisition and analysis.

Phylogenetic delineation using MLSA

Three housekeeping genes, *cts* (citrate synthase), *gyrB* (DNA gyrase B), and *gapA* (glyceraldehyde-3-phosphate), were sequenced for MLSA to place strains into their phylogroups and assess diversity. The *cts* gene alone is sufficient to place an isolate in its respective phylogroup in the *P. syringae* species complex and thus was used for phylogenetic placement in this study (Berge et al. 2014). For deeper resolution of phylogenetic relationships, *gyrB* and *gapA* were also sequenced and used in concatenation with the *cts* gene for MLSA. The primers used for amplifying DNA and for Sanger sequencing of *gyrB*, as well as PCR conditions, were based on those of Hwang et al. (2005), and the primers for *gapA* and *cts* amplification and sequencing were based on that of Morris et al. (2008). PCR product purification and Sanger sequencing were performed by Genewiz (South Plainfield, NJ).

Geneious Prime 2021.1.1 software was used to assemble, trim, and align all sequences for the MLSA. Forward and reverse sequences from each reaction were aligned as contigs and trimmed according to Hwang et al. (2005) or Morris et al. (2008). The trimmed fragment lengths were 427 bp for *cts,* 507 bp for *gyrB*, and 476 bp for *gapA*. The sequences of each locus were concatenated in the order of *cts-gyrB-gapA* and created a final concatenated sequence length of 1,410 bp. Concatenations were pairwise aligned to one another. Reference sequences were obtained from the Plant Associated and Environmental Microbes database (Almeida et al. 2010) or NBCI. Model testing was conducted on concatenated loci in CLC Main Workbench 7 (Qiagen, Hilden, Germany). The general time-reversible model was used in tree construction. The Geneious MrBayes plugin was used to create a Bayesian tree with a general time-reversible tree (Huelsenbeck and Ronquist 2001).

Analysis of molecular variance (AMOVA) and population structure analysis

An AMOVA test was performed to infer the distribution of genetic diversity among and within PG2b subpopulations (Excoffier et al. 1992). Seven subpopulations, based on the area of sample collection and with a minimum of five strains were considered as follows: Klamath Falls, OR (5); Shasta Valley, CA (7); St. Paul, MN (8); Susanville, CA (15); Scott Valley, CA (22); Tulelake, CA (9); and Cornish, UT (18) (Supplementary Table S2). PG7a subpopulations were not analyzed due to the low number of strains. The Phi (Φ) statistic was used to infer subpopulation differentiation under the null hypothesis (H_0) of no differentiation. Statistical significance was tested with a permutation procedure (999 permutations). Analyses were done with and without clone-censored strains by col-

lection sites. Population structure was also analyzed by randomly shuffling the strains by subpopulations. The analysis was carried out using the poppr package (v.2.9.3; Kamvar et al. 2014) with a modified script provided by Cory Hirsch, Department of Plant Pathology, University of Minnesota, under the RStudio environment (v.4.1.0).

Genome sequencing, annotation, and analysis

Twelve *P. syringae* (PG2b-grouping) strains and eight *P. viridiflava* (PG7a-grouping) strains were chosen for whole-genome sequencing from the collection of 94 PG2b strains and 29 PG7a strains. These strains were selected based on characteristics including geographic location of isolation and pathogenic potential on alfalfa. The PG2b strains with relatively high aggressiveness were Susan2139, U643, KF529, and SV1599; moderately aggressive strains were T230, SV1866, STP26, and T1434; and the least aggressive strains were SV921, SV323, U888, and Susan762. Selected PG7a strains with higher aggressiveness were STP3 and T157; moderately aggressive strains were SV1779, U658, and U625; and the least aggressive strains were KF2185, T1426, and STP4. The strains were grown with shaking at room temperature in LB liquid medium for 48 h, pelleted, washed with sterile distilled water, and submitted to the Microbial Genome Sequencing Center (Pittsburgh, PA) for DNA extraction, library preparation, and whole-genome sequencing and annotation. DNA extractions were performed with the DNeasy Blood & Tissue Kit (Qiagen), and the Illumina DNA Prep Kit (Illumina, San Diego, CA) and Oxford Nanopore Ligation Sequencing Kit were used for library preparation. Samples were run on NextSeq 550 (Illumina), which provided $2\times$ 150-bp paired end reads, and MinION (Oxford Nanopore Technologies, Oxford, U.K.; ONT) sequencers to obtain short- and long-read DNA sequences, respectively. Hybrid assembly of Illumina and ONT reads was performed with Unicycler (v0.4.8). Genome sequences were deposited in the NCBI genome database and annotated via the Prokaryotic Genome Annotation Pipeline. An announcement of the availability of the assembled genome sequences and their main features has been published (Lipps et al. 2022). For single virulence gene analyses, gene sequences were extracted and aligned, and Bayesian trees were created using Geneious Prime Software version 2021.1.1.

Results

Isolation and identification of strains

A total of 2,612 (73.0%) out of 3,575 of the alfalfa stems that were processed in 2016, 2017, 2019, and 2020 were ice-nucleation (INA) positive (Supplementary Table S1). A collection of 260 PG2 strains and 107 PG7 strains were isolated from the INA-positive stems. For further genetic and phenotypic analyses, 94 PG2 and 29 PG7 strains were selected, and phylogenetic placement was confirmed by sequencing of the *cts* gene (Supplementary Table S2). All PG2 strains were identified as belonging to PG2b, and all PG7 strains belonged to PG7a from analysis of *cts.*

Aggressiveness of PG2b strains was greater than PG7a strains

Strains were tested for their ability to cause disease on the susceptible alfalfa cultivar CUF101 using a wounded stem inoculation assay. Disease ratings on stems and leaves from 1 to 5 (1 = no disease; 5 = systemic chlorosis and necrosis; Fig. 1) were assigned to each plant replicate, and the average disease scores for stems and leaves were calculated. Symptoms caused by PG2b strains were indistinguishable from those caused by PG7a strains. The Pearson correlation coefficient describing the relationship between leaf and stem scores was calculated and showed a moderately positive correlation ($r = 0.409$).

There was a large range in mean disease scores for individual *P. syringae* PG2b strains, from 1.8 to 4.7 on leaves and 1.2 to 4.5 on stems. Similarly, there was a large range in scores for *P. viridiflava* PG7a strains, from 1.4 to 4.0 on leaves and 1.0 to 2.5 on stems

(Fig. 2). The average stem disease score caused by all *P. syringae* PG2b strains was 2.7, and the average leaf score was 3.4. For all *P. viridiflava* PG7a strains, the average stem score was 2.0 and the average leaf score was 2.8. Overall, *P. syringae* PG2b strains incited significantly greater disease scores on stems ($P = 4.9\text{E-}12$) and leaves ($P = 2.2\text{E-}06$) than those caused by *P. viridiflava* PG7a strains (Fig. 2).

Two-way ANOVA tests were performed to explore the impact of location and species on stem and leaf scores using data from strains from Tulelake, Scott Valley, Susanville, Shasta Valley, and Cornish (72 PG2b strains and 25 PG7a strains). Strains from St. Paul, Klamath Falls, South Charleston, and Shasta Valley were omitted from this analysis, as there were not enough representative strains for each location to conduct the statistical analysis. The analyzed data were normally distributed and of equal variances. There were no significant differences between average leaf scores ($P = 0.31$) or stem scores ($P = 0.16$) caused by PG2b and PG7a strains from different locations, nor was there a significant compounding impact of species and location on leaf score ($P = 0.25$) or stem score ($P = 0.23$) (data not shown). As expected, there were significant differences by species in the leaf score ($P = 2.4\text{E-}05$) and stem score ($P = 3.7\text{E-}11$).

Double inoculation assays were conducted in which alfalfa plants were inoculated with a mixture of *P. syringae* PG2-grouping strains and *P. viridiflava* PG7-grouping strains. Four strains of PG2b (U888, Susan2121, T1434, and T1207) and four strains of PG7a (KF485, U625, StP3, and SV1796) characterized as mid-level aggressiveness were tested individually and then combined (T1207 + SV1796, StP3 + U888, KF485 + T1434, Susan2121 + U625). A one-way ANOVA test indicated no significant difference in the average disease scores on stems ($P = 0.079$) or leaves ($P = 0.26$) among plants inoculated with both pathogens compared with a single pathogen (Supplementary Fig. S1).

Ice nucleation frequency is high in PG2b strains but absent in PG7a strains

A strain was defined as ice nucleation active if the average concentration of a frozen sample at $-4.5°C$ was 1×10^6 CFU/ml or less. Of all isolates tested, 59 of 94 (63%) *P. syringae* PG2-grouping strains were INA, and none of the 30 *P. viridiflava* PG7 strains was INA (Supplementary Table S2). The distribution of INA-positive or -negative strains varied among locations. The highest frequency of INA was for strains from Tulelake (100%; 9/9 strains) and the lowest for St. Paul strains (0%; 0/9 strains). Strains from Shasta Valley (17%;1/6) and Klamath Falls (33%; 2/6) also had a low frequency of INA. Strains from Susanville (75%; 12/16), Scott Valley (73%; 19/26), and Cornish (71%; 15/21) all had relatively high frequencies of INA. ALF3, the reference BSB strain from Wyoming, was also INA.

Differential host responses to PG2b and PG7a strains

Plants inoculated with the PG2b strain SV921 showed a host reaction within the xylem, pith parenchyma, and chlorenchyma cells up to 0.75 cm from the wound site (Fig. 3). PG7a strain
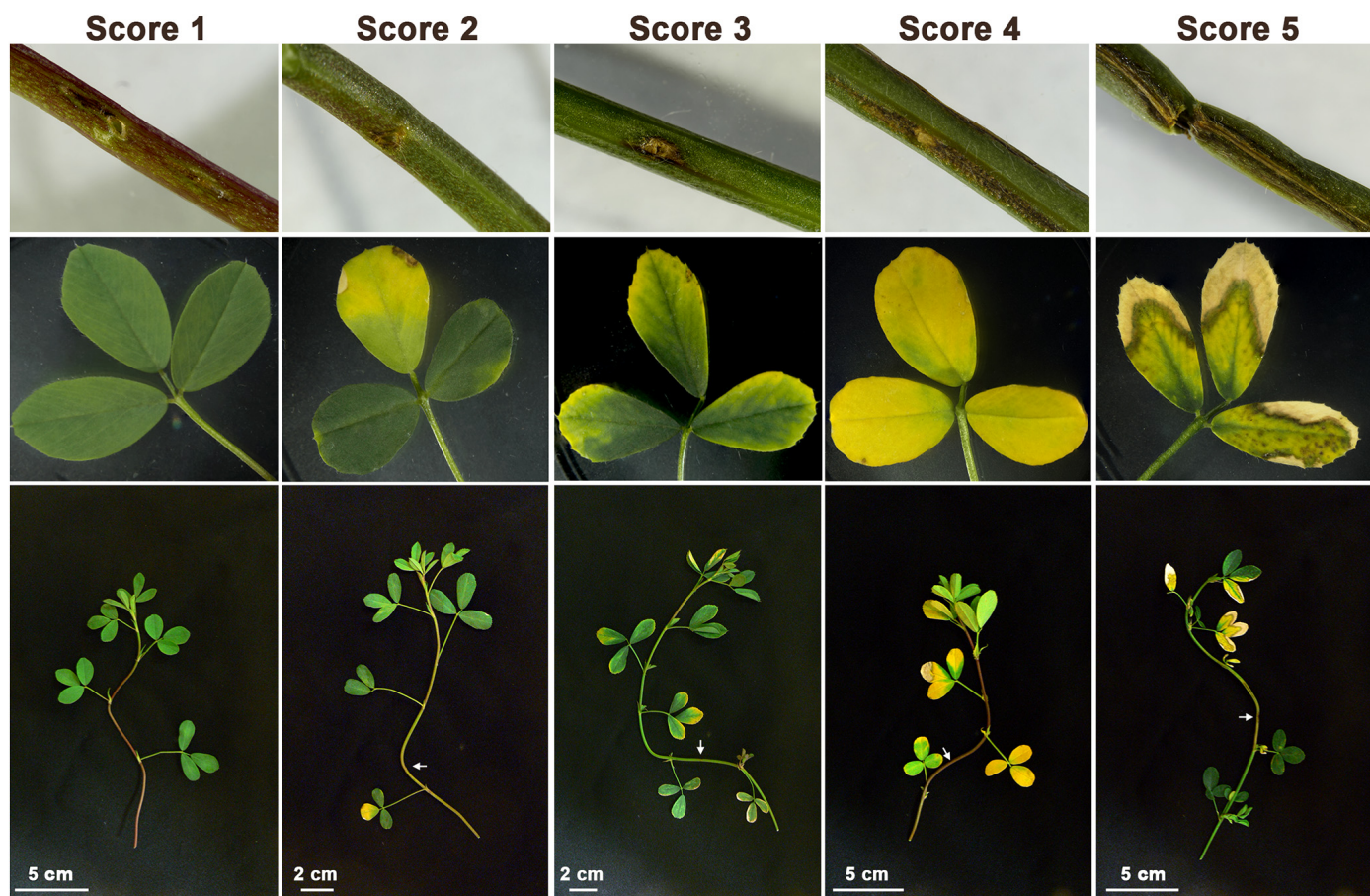
Fig. 1. Disease symptoms on leaves and stems of alfalfa inoculated with PG2b and PG7a strains. Stems were wounded with a tuberculin needle and bacteria at optical density at 600 nm (OD_{600}) = 0.1 ($\sim 1 \times 10^8$ CFU/ml) were applied with a sponge. Symptoms were rated 7 to 10 days after inoculation. 1 = no necrosis on stem, no symptoms on leaves; 2 = minimal browning at wound site, leaf symptoms limited to one node; 3 = lesion extends from wound site <5 mm, yellowing on leaves on two or more nodes; 4 = lesion extends >5 mm from wound site, yellowing of leaves is systemic; and 5 = lesion causes stem collapse/breakage, leaf necrosis with defoliation.

Tule157 also caused discoloration in the xylem, pith parenchyma, and chlorenchyma cells above the wound site. Collapse of epidermal cells and disintegration of the pith parenchyma cells were much more pronounced with infection by PG2b strain SV921 compared with the response to PG7a strain Tule157. Plants mock-inoculated with water did not display a reaction within the xylem cells above the wound site.

MLSA identified high levels of diversity within PG2b and PG7a strains

The *cts* housekeeping gene was sequenced for 94 PG2b and 29 PG7a strains, and the sequences were aligned with reference *cts* sequences from representative strains of each phylogroup in the *P. syringae* complex. The strains from alfalfa grouped exclusively with PG2b and PG7a as anticipated (Supplementary Fig. S2). For further analysis of the diversity of strains within each phylogroup, MLSA was conducted using the concatenated sequences of *cts*, *gapA*, and *gyrB* of alfalfa strains, as well as reference strains of *P. syringae* complex phylogroups used by Berge et al. (2014) (Fig. 4). The Bayesian tree created from concatenated sequence alignments resulted in the same grouping of isolates in PG2b and PG7a but showed more fine-tuned relationships and groupings of isolates within their respective phylogroups. The MLSA-based Bayesian tree was supplemented with phenotypic data including disease scores on leaves and stems of each strain in this study, as well as INA. The PG2b strains in this study grouped with PG2b reference strains *P. syringae* pv. *japonica* M301072 (barley pathogen) and *P. syringae* pv. *pisi* H5E1 (pea pathogen). PG7a strains in this study grouped with PG7a reference strains CMO0085 and CC1582. Haplotypes were assigned to all but 12 strains in this study based on the concatenated sequences of *cts*, *gyrB*, and *gapA*. Each concate-

nated sequence with at least one base pair difference was assigned as a unique haplotype (Supplementary Table S2). There were 42 sequence types of PG2b strains out of a total of 94 PG2 strains. Each of the PG7b strains evaluated ($n = 19$) represented a unique sequence type (10 of the 29 PG7 strains were not subjected to sequence typing). Several PG2b haplotypes were present in different locations. For example, haplotype 8 had strains from five locations, followed by haplotypes 1, 7, 34, and 47 with strains from three locations (Supplementary Fig. S3). Haplotype 7 was the most frequently identified haplotype, with 10 strains. Locations varied in their number of unique haplotypes; for example, the Scott Valley location harbored 30 haplotypes and Cornish harbored 24, even though the total number of strains from each location was comparable. Some sequence types had higher disease scores on stems or leaves than others. However, the pathogenic potential by sequence type cannot be accurately compared because some sequence types only were represented by one strain, whereas some were represented by up to 10 strains. Although there were some haplotypes with a greater percentage of INA strains (haplotypes 1, 7, 12, 46) and some with lower percentages of INA capacity (haplotypes 9, 34), they cannot be statistically compared due to low and differing amounts of stains per sequence type.

## Subpopulation differentiation and genetic structure analysis of PG2b strains

AMOVA on strains from seven locations indicated that most of the genetic variation occurred within the subpopulations from each location. The analysis without clone censoring indicated a slight differentiation among subpopulations that explained about 5.9% of the variation ($\Phi = 0.059$; $P = 0.001$), whereas the analysis with clone correction indicated no subpopulation differentiation ($\Phi = -0.018$; $P = 1.000$) (Supplementary Table S3; Supplementary Fig. S4). No population structure was detected within the PG2b strains ($\Phi = 0.005$; $P = 0.259$) (Supplementary Fig. S4).

Genomic sequence comparison

The genomes of 12 PG2b and 8 PG7a strains representative of varied virulence capacities and locations were sequenced and assembled. Detailed metrics for each genome are published (Lipps et al. 2022). Using the genome sequences, a more robust MLSA was performed using seven housekeeping genes that make up the core genome of *P. syringae*: *acn1*, *cts*, *gapA*, *pgi*, *rpoD*, *gyrB*, and *pfk* (Sarkar and Guttman 2004). Strain grouping in the seven-gene MLSA phylogenetic tree was nearly identical to the placements in the three-gene MLSA (Fig. 5).

The presence/absence of the following virulence factor genes found within PG2b and/or PG7a were investigated: *inaZ* (ice nucleation), *gacA/gacS* (syringolin A), *corA* (coronatine), *sypA* (syringopeptin), *syrB1/B2* (syringomycin), *avrE*, *hopaa1/hopPsyA*, *hopaj2* (avirulence effectors), *hrpZ/hrpA/hrpW* (T3SS outer proteins), and *pel* (pectate lyase). The sequences for *hrpZ*, *hrpA*, and *hrpW*, as well as *avrE*, were identified in all genome assemblies. All 12 PG2b strains in this study contained the selected virulence genes (excluding *pel*, which is specific to PG7a), except for the lack of *sypA* in T230 and T1434 (moderate pathogenicity) and in SV1599 and Susan2139 (high pathogenicity). Likewise, Susan2139 did not contain the *syrB1B2* gene. None of the PG7a strains contained the *inaZ* gene, corroborating the INA-negative phenotypes of these strains. All PG7a strains and none of the PG2b contained the *pel* gene, as predicted by typical strain phenotypes.

The *hrcC* gene, a conserved portion of the T3SS required for virulence, was analyzed for of PG7a strains and used to build a Bayesian tree (Fig. 6) with reference strains containing S-PAI or T-PAI (Bartoli et al. 2014) to determine the type of PAI in strains from this study. All *hrcC* genes from PG7a alfalfa strains in this study grouped with S-PAI reference strains.
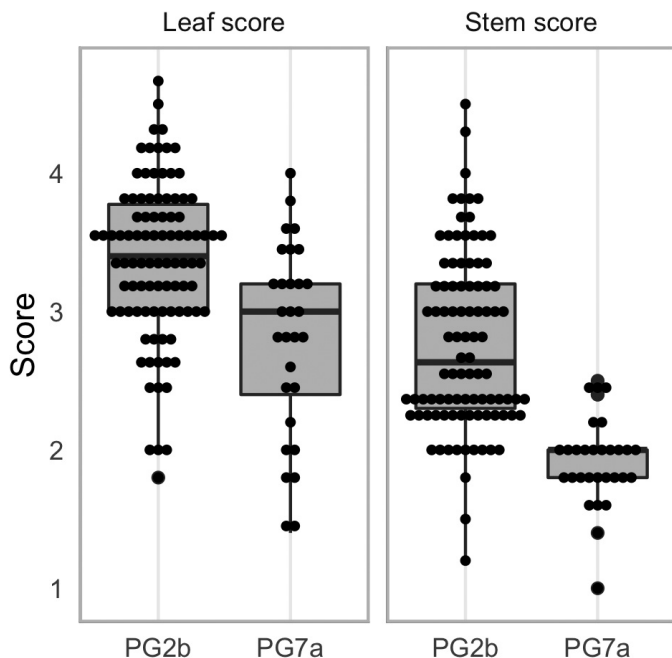
Fig. 2. Leaf and stem disease scores by phylogroup. For each strain in this study, six alfalfa plants were inoculated, and leaf and stem disease scores on a 1-to-5 scale were recorded 7 to 10 days postinoculation. 1 = no necrosis on stem, no symptoms on leaves; 2 = minimal browning at wound site, leaf symptoms limited to one node; 3 = lesion extends from wound site <5 mm, yellowing on leaves on two or more nodes; 4 = lesion extends >5 mm from wound site, yellowing of leaves is systemic; and 5 = lesion causes stem collapse/breakage, leaf necrosis with defoliation. The average scores of the six replicates were calculated for each strain. The upper limit of the boxes represents the third quartile, and the lower limit of the boxes represents the second quartile. The middle bar in the boxes represents the median. Individual points represent the average disease score of each strain.

Discussion

This is the first comprehensive characterization of PG2b and PG7a strains causing BSB on alfalfa, an important disease emerging in various locations within the United States. Based on the data presented here, BSB is a disease involving multiple genetic lines within the *P. syringae* species complex. All strains characterized in this study were identified as either *P. syringae* PG2b or *P. viridiflava* PG7a, known contributors to BSB. It is possible that the species diversity of bacteria involved in BSB is greater than what was reported here. For example, alfalfa with BSB symptoms from California also had abundant populations of *P. marginalis*, a member of the *P. fluorescens* group, which caused small stem lesions, but not chlorosis or necrosis, when inoculated into alfalfa stems (D. A. Samac, *unpublished data*). Future research could utilize a general probe for the entire *P. syringae* group such as that described by Guilbaud et al. (2016) to avoid bias in identification of BSB pathogens. Overall, the results show that both pathogens, PG2b and PG7a, are genetically and phenotypically diverse across a broad geographical area, and the same haplotypes were found on alfalfa plants separated by thousands of kilometers, indicating that it is unlikely that a recent introduction or evolution of more aggressive strains is the basis for recent emergence. Changes in crop germplasm, crop management, or environmental shifts may have played a role in increasing incidence of BSB. This result is consistent with the suggestion of Morris et al. (2022) that surveillance for disease outbreaks due to environmentally ubiquitous *P. syringae* lines with high pathogenic potential should focus on changes in environmental condition and cropping practices more so than any specific biological trait of the strains. In addition to monitoring environmental and cultural factors, surveillance of BSB disease outbreaks may also involve the screening for presence of PG2b and PG7a strains by genetic sequencing of the *cts* gene, as these are the currently known causal agents. If future research reveals additional *P. syringae* strains involved in causing BSB, they may be used for screening/diagnosis of this disease as well.

P. syringae PG2b strains caused higher stem and leaf scores than *P. viridiflava* PG7a strains on alfalfa (Supplementary Table S2; Fig. 2). This corroborates literature reports that *P. viridiflava* is generally a less aggressive, opportunistic pathogen (Bartoli et al. 2014). In our study, *P. viridiflava* PG7a strains were able to induce leaf and stem symptoms in most cases, although there was some variation in virulence, with some strains causing only mild disease

symptoms (disease scores between 1 and 2), whereas others caused severe symptoms (disease scores up to 4). Likewise, although *P. syringae* PG2b strains on average induced higher disease scores on both stems and leaves, there was variability in the average level of disease caused by different strains. Taken together, these findings agree with those of Morris et al. (2019) that there can be variability within disease-inducing potential among strains in the same phylogroup or sub-phylogroup of *P. syringae*. Differences in virulence among strains within the same phylogroup may be attributed to macro- (e.g., field and greenhouse) or micro-environmental (e.g., growth chamber) factors, such as temperature and humidity fluctuations or genetic and physiological differences among strains, such as different gene content, differential gene expression, secretion of effectors, or differences in bacterial enzymatic activity. Genetic variation among individual inoculated host plants may also contribute to variation in disease scores because alfalfa is a highly heterogeneous species. A study on the phenotypic and genotypic heterogeneity of *P. syringae* PG2b strains associated with alfalfa leaf spot in Iran also found that strains varied in pathogenicity on alfalfa and nine other hosts tested (Ansari et al. 2019). The strains from Iran cause somewhat different symptoms and appear more diverse by MLSA than those from the United States, although some Iranian strains cluster with the strain ALF3 from Wyoming.

Symptoms of BSB of alfalfa consist of blight lesions on stems and leaves, systemic chlorosis and necrosis of leaves, defoliation, and wilt and collapse of the stem. The development of BSB in the field begins with lesions on the stem near the axils, likely a site of frost damage, and therefore a bacterial entry point. The stems appear water soaked, yellow to olive green along the side of infection, and the leaves attached to the diseased portion of the stem exhibit yellowing along the midrib of the leaflets (Sackett 1910). Leaves are also infected directly and show water soaking followed by necrosis, chlorosis, and abscission from the stem. In this study, microscopic observation of disease symptoms shed light on lesion development once that the bacterium is within the plant. Plants were inoculated with either PG2b strain SV921 or PG7a strain Tule157 to compare potential qualitative differences in the infection and disease progression of the two strains from different phylogroups. Plants inoculated with the PG2b strain SV921 showed a reaction to the bacterium in the xylem, pith parenchyma, and chlorenchyma up to 0.75 cm away from the wound site (Fig. 3). Inoculation with PG7a strain Tule157 also resulted in discoloration in the xylem, pith parenchyma, and chlorenchyma cells above the wound site,
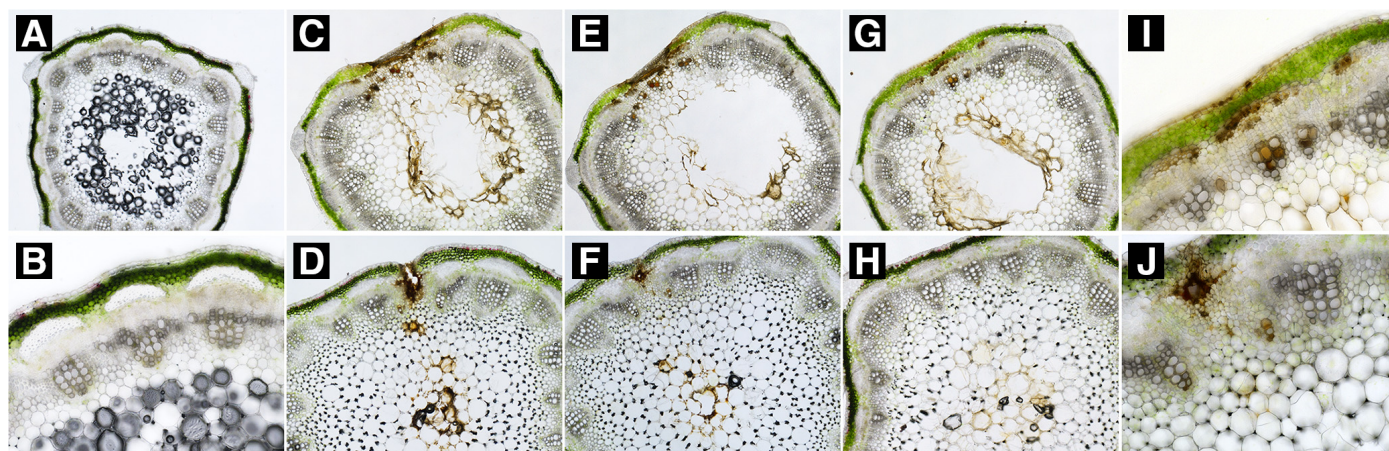

Fig. 3. Infection strategies differ due to PG2b and PG7a infection. Discoloration of xylem and chlorenchyma cells occurred with both strains with great collapse of epidermal and pith parenchyma by PG2b infection. Brightfield color images of cross sections of alfalfa stems from 100 to 700 μm above the inoculation points. **A,** Mock-inoculated control, 40×. **B,** Mock-inoculated control, 100×. **C,** 100 μm above the site of inoculation with PG2b strain SV921, 40×. **D,** 100 μm above the site of inoculation with PG7a strain Tule157, 40×. **E,** 300 μm above the cross section shown in C. **F,** 300 μm above the cross section shown in D. **G,** 300 μm above the cross section shown in E. **H,** 300 μm above the cross section shown in F. **I,** Magnification of discoloration from the section shown in E, 100×. **J,** Magnification of discoloration from the section shown in F, 100×.

although to a lesser extent, and the reaction was not observed in the chlorenchyma cells at the farthest point from inoculation. This indicates that the pathogen may enter the xylem during infection, damaging the xylem cells and/or triggering plant reactions, then moving into the xylem, and potentially blocking flow within the xylem as the infection progresses. Additionally, in a preliminary study, we showed that in alfalfa plants inoculated with GFP-labeled *P. syringae*, the bacteria are present within the vasculature (D. A. Samac, *unpublished data*). Blocked xylem vessels due to infection may contribute to the chlorosis and necrosis symptoms in the leaves. Degradation of pith parenchyma is likely the cause of stem collapse and stem breakage observed in severe BSB infections. In addition to blockages within the plant vasculature, phytotoxins are major virulence factors for *P. syringae* pathogens (Bender et al. 1999). The arsenal of phytotoxins produced by this pathogen likely also contribute to chlorosis and necrosis.

All sequenced BSB PG2b strains had virulence genes *gacA/gacS* (syringolin A) and *corA* (coronatine), whereas 4 of 12 were lacking *sypA* (syringopeptin), and one lacked *syrB1/B2* (syringomycin) (Fig. 5). However, the lack of toxin genes did not seem to affect aggressiveness. For example, Susan2139 lacked *syrB1/B2* but maintained a mean leaf score of 4.6 and stem score of 2.5. The ability of *P. syringae* PG2 strains to colonize xylem vessels postinoculation has been demonstrated in the model plant *Nicotiana ben-*

thamiana (Misas-Villamil et al. 2013). In that study, plants were inoculated with *P. syringae* pv. *syringae* PG2d strains, including a GFP-containing strain and a mutant deficient in the syringolin gene, *sylC*. Within 5 days, the GFP-containing strain was detected within the vasculature above the point of inoculation. Furthermore, at that same time point, the *sylC* deficient strain had a lower rate of wound entry (Misas-Villamil et al. 2013). Given these data and the importance of toxins in the infection process of *P. syringae*, it seems likely that toxins play a role in successful colonization of the alfalfa stem; however, it will be necessary to evaluate the quality and quantity of toxin production to properly assess its correlation with BSB disease severity. Additionally, specific fluorescent antibodies have been used to successfully detect syringomycin on the periphery of pith parenchyma cells in peach trees after inoculation with purified toxin (Paynter and Alconero 1979). It is likely that in the case of the SV921 infection, syringomcyin and/or syringopeptin may have been responsible for the deterioration of the pith parenchyma cells, as well as involved in systemic necrosis (Gross and DeVay 1977). Coronatine mimics the action of the phytohormone jasmonic acid and can inhibit salicylic acid accumulation, which reduces plant defense responses against some microorganisms (Zheng et al. 2012). Coronatine also causes chlorosis in hosts of *P. syringae* pv. *tomato* (Bender et al. 1987). The identification of *corA* in the genome of PG2b strains is unusual (Baltrus et al. 2011) and warrants further
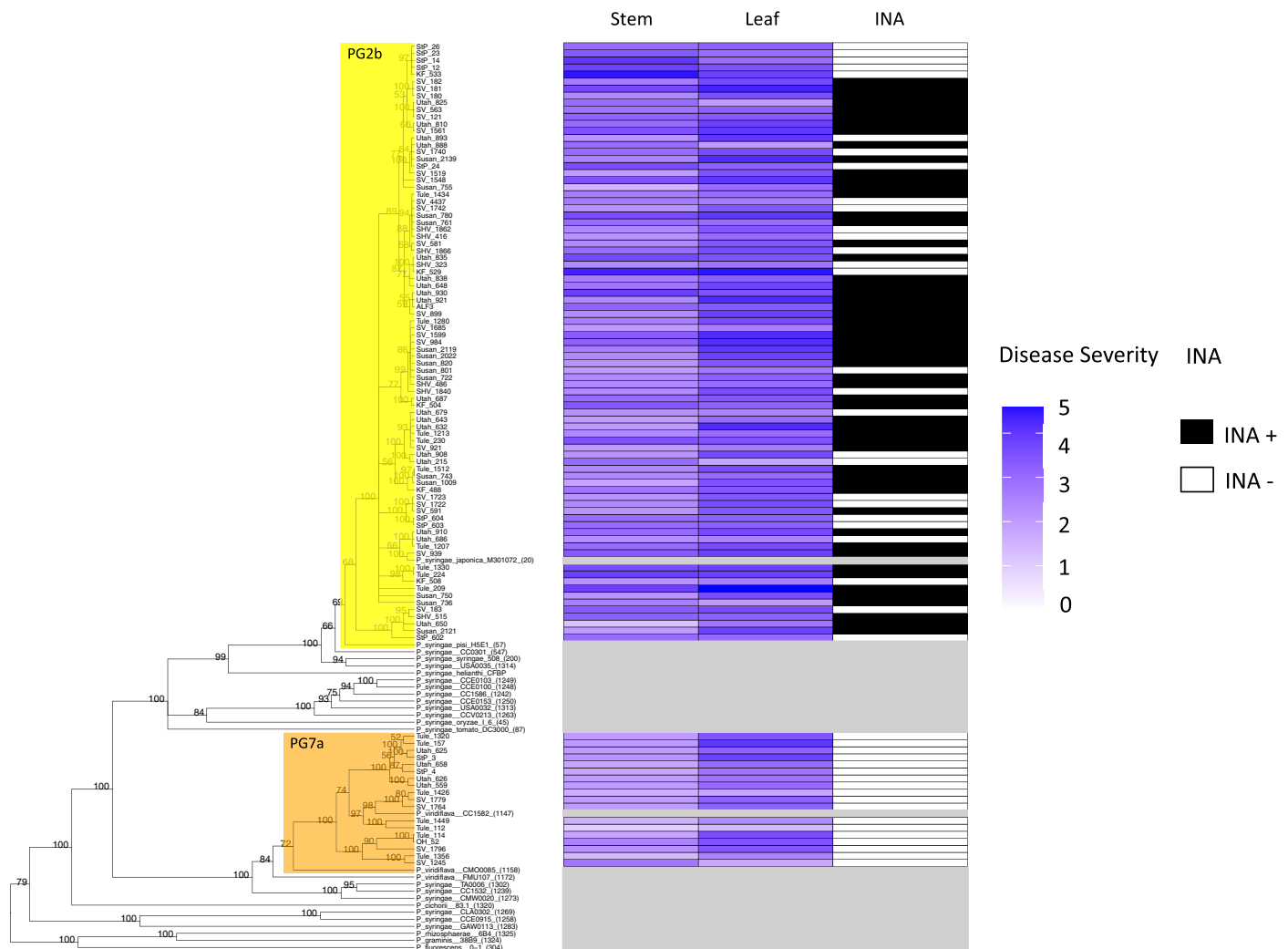
Fig. 4. Bayesian tree of concatenated *cts*, *gyrB*, and *gapA* genes of PG2b and PG7a strains causing bacterial stem blight. The tree was constructed with reference strains from *Pseudomonas syringae* phylogroups defined by Berge et al. (2014). Average disease scores on stems and leaves of alfalfa and ice nucleation activity (INA) are presented. Gray boxes indicate no data for reference strains.

investigation for a possible role of coronatine in pathogenicity of BSB strains.

Infection with PG7a Tule157 also resulted in discoloration of xylem vessels, but to a lesser extent than inoculation with SV921, and degradation of pith parenchyma cells up to 0.75 cm above the inoculation site (Fig. 3). One of the most notable virulence strategies of *P. viridiflava* is expression of pectate lyase to degrade primary cell walls. At maturity, xylem vessels form tough, lignified secondary cell walls. However, pith parenchyma cells do not form secondary cell walls and thus are a target for pectate lyase resulting in cell maceration and lysis. It is likely that in the case of the PG7a Tule157 inoculation, the strain utilized pectate lyase enzyme (*pel*) to macerate the pith parenchyma. The decreased ability of the PG7a strain to colonize xylem compared with PG2b strains may explain why *P. viridiflava* strains generally showed less severe symptoms on alfalfa. Xylem colonization may be important for the moderate to severe development of BSB symptoms.

The MLSA identified several unique haplotypes that were present in different locations, as well as locations with unique haplotypes.

There has been little research into the epidemiology of BSB, although there is extensive knowledge of the movement of *P. syringae* in the environment. At the landscape scale, *P. syringae* is carried by rain and snowfall and survives in snowpack on the ground, and it can move into river networks and irrigation waters and exist in epilithic biofilms in aquatic environments (Morris et al. 2013). Cells of *P. syringae*, including BSB pathogens that are moved by these processes, would be able to colonize the alfalfa phyllosphere, and under conducive conditions, they could cause disease. Our data suggest that the PG2b strains are mobile in continental or larger water systems. This is reinforced by the lack of subpopulation differentiation (and structure) of haplotypes within the PG2b strains. Using a standard assay, of all strains tested, 63% of the *P. syringae* PG2b-grouping strains were INA, whereas the gene was absent in all the *P. viridiflava* PG7a-grouping strains analyzed. In other studies, most PG2 strains (85%) were reported to be INA, whereas a much lower percentage of PG7 strains (around 30%) were INA positive (Bartoli et al. 2014; Berge et al. 2014). Because *inaZ* was found in the genome of all PG2b strains sequenced, even those that tested
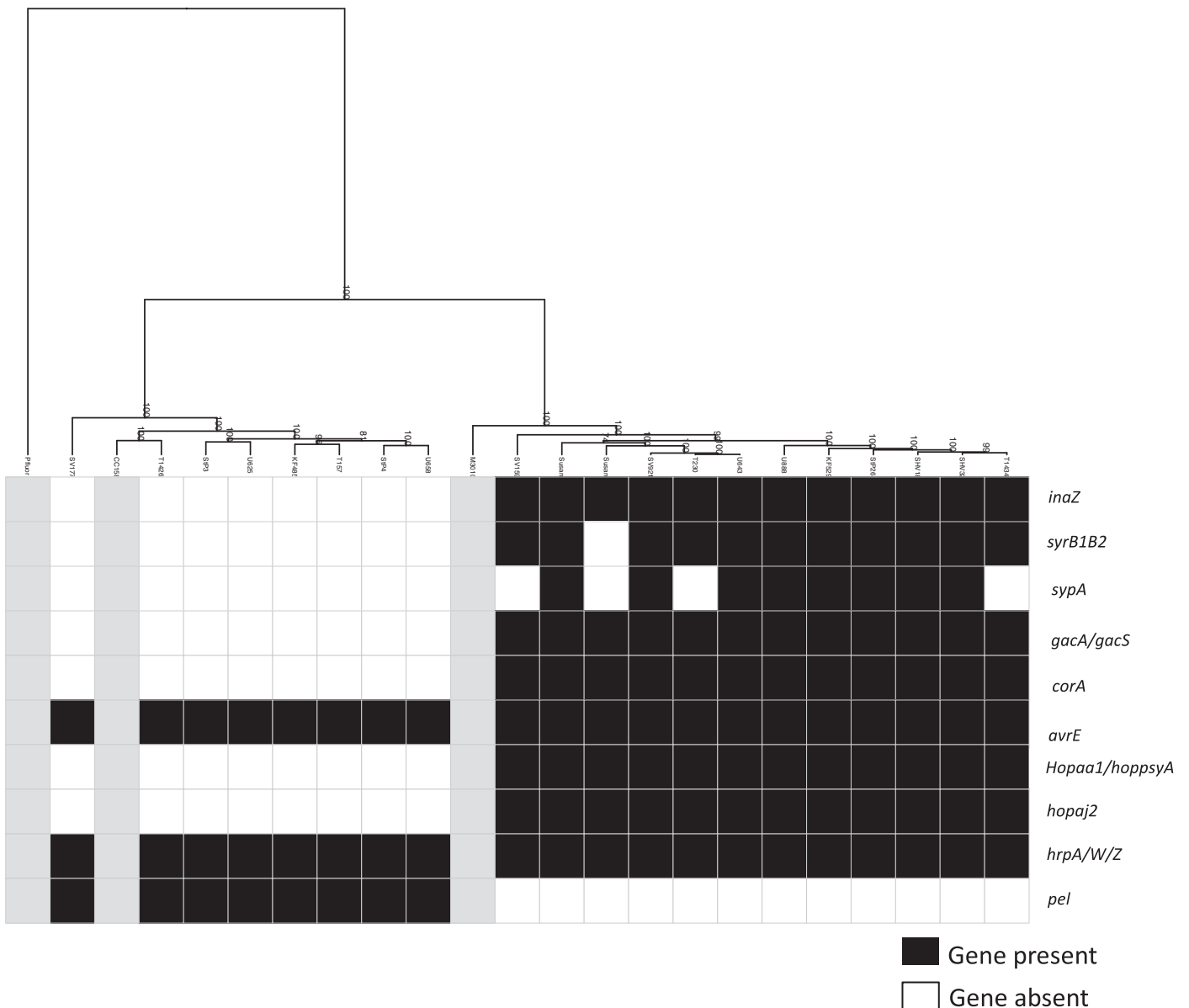

Fig. 5. Seven-gene multilocus sequence analysis Bayesian tree of PG2b and PG7a strains. The tree was constructed from the alignment of the core genome gene sequences *acn1*, *cts*, *gapA*, *pgi*, *rpoD*, *gyrB*, and *pfk*. The presence or absence of genes is displayed for each strain. Reference sequences that were not part of this study are represented with gray boxes.

INA negative, it is possible that the cold induction period was too short or that the ice protein expression is lower in alfalfa isolates than in other PG2b strains. Furthermore, the test in this study used a relatively warm cutoff temperature for freezing; further testing at temperatures down to $-8°C$ could be done to reveal potentially more INA strains. Because most strains in the PG2b population causing BSB are INA, it is reasonable that INA capability provides an advantage to this pathogen in causing BSB in alfalfa in the field, promoting frost injury and thus providing an entry point into the plant. Research to test INA and pathogenicity under low temperature conditions that mimic field conditions of BSB is needed to understand the role of INA in BSB disease. Although PG7-grouping isolates generally have less INA potential than PG2-grouping isolates, it was surprising that in this study, none of the 29 PG7a strains met the criteria for INA, and none of the sequenced strains had the *inaZ* gene. However, several strains were INA positive at higher concentrations of 1×10^7 or 1×10^8 CFU/ml, indicating the presence of *inaZ* in some alfalfa PG7a strains.

A unique aspect of BSB of alfalfa is the identification of two bacterial species in infected plants, each of which cause simi-

lar symptoms under controlled environmental conditions. Lukezic et al. (1983) reported isolation of *P. viridiflava* from diseased alfalfa crowns and showed it to cause crown rot and root rot under controlled conditions. The bacterium was also isolated from roots of wilted alfalfa plants from Iran and shown to cause stunting and wilting when inoculated into alfalfa stems (Heydari et al. 2012). We consistently isolated both *P. syringae* PG2b and *P. viridiflava* PG7a from alfalfa stems with BSB symptoms, demonstrating that *P. viridiflava* infects aerial portions of the plant and causes disease. Although disease complexes have been recognized for many plant hosts, the individual contributions of members of the complex to disease and possible synergistic interactions have rarely been investigated (Lamichhane and Venturi 2015). The advent of next-generation sequencing has led to the growing awareness of multiple microbes associated with an individual host. The concept of one microbe-one disease is starting to be reevaluated and replaced with the principle of the pathobiome, a comprehensive biotic environment that includes a diverse community of all disease-causing organisms within the plant and defines their mutual interactions and the resultant effect on plant health (Bass et al. 2019). We tested for
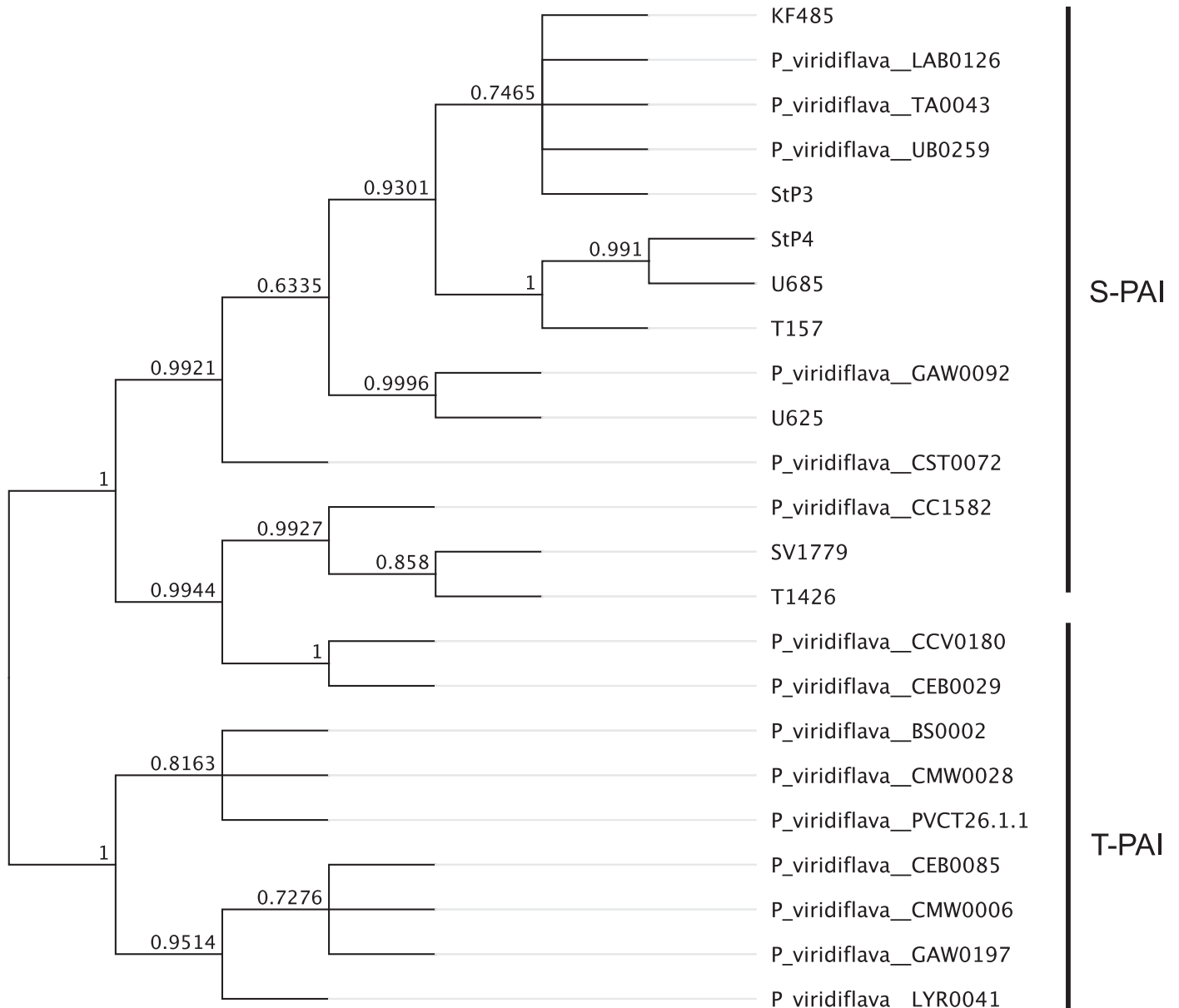
Fig. 6. A Bayesian tree of the *hrcC* sequences of PG7a strains in this study. Numbers on nodes denote bootstrap values.

synergism between the two alfalfa BSB pathogens, expecting that the different virulence mechanisms would be complementary and result in greater disease symptoms. Surprisingly, when PG2b and PG7a strains were coinoculated into alfalfa stems, there appeared to be a lack of synergy and no change in disease symptoms compared with inoculation with a single strain (Supplementary Fig. S1). It is possible that field conditions may favor a positive interaction and thus synergy among those two species. Alternatively, the two bacteria may interact antagonistically. Additional experiments under varying conditions and inoculum densities using marked strains are needed to tease apart the potential interactions between the two pathogens. Also, a more in-depth comparison of genomes and bacterial transcripts may shed light on genes specifically involved in causing disease on alfalfa. Nonetheless, the occurrence of two pathogens causing BSB needs to be considered when developing resistant cultivars and overall disease control measures.

Literature Cited

Almeida, N. F., Yan, S., Cai, R., Clarke, C. R., Morris, C. E., Schaad, N. W., Schuenzel, E. L., Lacy, G. H., Sun, X., Jones, J. B., Castillo, J. A., Bull, C. T., Leman, S., Guttman, D. S., Setubal, J. C., and Vinatzer, B. A. 2010. PAMDB, a multilocus sequence typing and analysis database and website for plant-associated microbes. Phytopathology 100:208-215.

Ansari, M., Taghavi, S., Zarei, S., Merhb-Moghadam, S., Mafakheri, H., Hamidizade, M., and Osdaghi, E. 2019. Phenotypically and genotypically heterogeneous strains of Pseudomonas syringae associated with alfalfa leaf spot disease in Iran. Plant Dis. 103:3199-3208.

Anzai, Y., Kim, H., Park, J. Y., Wakabayashi, H., and Oyaizu, H. 2000. Phylogenetic affiliation of the pseudomonads based on 16S rRNA sequence. Int. J. Syst. Evol. Microbiol. 50:1563-1589.

Baltrus, D. A., McCann, H. C., and Guttman, D. S. 2017. Evolution, genomics and epidemiology of Pseudomonas syringae: Challenges in bacterial molecular plant pathology. Mol. Plant Pathol. 18:152-168.

Baltrus, D. A., Nishimura, M. T., Romanchuk, A., Chang, J. H., Mukhtar, M. S., Cherkis, K., Roach, J., Grant, S. R., Jones, C. D., and Dangl, J. L. 2011. Dynamic evolution of pathogenicity revealed by sequencing and comparative genomics of 19 Pseudomonas syringae isolates. PLoS Pathog. 7: e1002132.

Bartoli, C., Berge, O., Monteil, C. L., Guilbaud, C., Balestra, G. M., Varvaro, L., Jones, C., Dangle, J. L., Baltrus, D. A., Sands, D. C., and Morris, C. E. 2014. The Pseudomonas viridiflava phylogroups in the P. syringae species complex are characterized by genetic variability and phenotypic plasticity of pathogenicity-related traits. Environ. Microbiol. 16:2301-2315.

Bartoli, C., Lamichhane, J. R., Berge, O., Varvaro, L., and Morris, C. E. 2015. Mutability in Pseudomonas viridiflava as a programmed balance between antibiotic resistance and pathogenicity. Mol. Plant Pathol. 16:860-869.

Bass, D., Stentiford, G. D., Wang, H.-C., Koskella, B., and Tyler, C. R. 2019. The pathobiome in animal and plant diseases. Trends Ecol. Evol. 34:996-1008.

Bender, C. L., Alarcón-Chaidez, F., and Gross, D. C. 1999. Pseudomonas syringae phytotoxins: Mode of action, regulation, and biosynthesis by peptide and polyketide synthetases. Microbiol. Mol. Biol. Rev. 63:266-292.

Bender, C. L., Stone, H. E., Sims, J. J., and Cooksey, D. A. 1987. Reduced pathogen fitness of Pseudomonas syringae pv. tomato Tn5 mutants defective in coronatine production. Physiol. Mol. Plant Pathol. 30:273-283.

Berge, O., Monteil, C. L., Bartoli, C., Chandeysson, C., Guilbaud, C., Sands, D. C., and Morris, C. E. 2014. A user's guide to a data base of the diversity of Pseudomonas syringae and its application to classifying strains in this phylogenetic complex. PLoS One 9:e105547.

Bookbinder, M. G., Bloom, J. R., and Lukezic, F. l. 1982. Interactions among selected endoparasitic nematodes and three Pseudomonads on alfalfa. J. Nematol. 14:105-109.

Bordjiba, O., and Prunier, J.-P. 1991. Establishment of an epiphytic phase by three species of Pseudomonas on apricot trees. Acta Hortic. 293:487-494.

Bricout, A., Morris, C. E., Chandeysson, C., Duban, M., Boistel, C., Chataigné, G., Lecouturier, D., Jacques, P., Leclère, V., and Rochex, A. 2022. The diversity of lipopeptides in the Pseudomonas syringae complex parallels phylogeny and sheds light on structural diversification during evolutionary history. Microbiol. Spectr. 10:e01456-22.

Bull, C. T., and Koike, S. T. 2015. Practical benefits of knowing the enemy: Modern molecular tools for diagnosing the etiology of bacterial diseases and understanding the taxonomy and diversity of plant-pathogenic bacteria. Annu. Rev. Phytopathol. 53:157-180.

Canaday, C. H., Wyatt, J. E., and Mullins, J. A. 1991. Resistance in broccoli to bacterial soft rot caused by Pseudomonas marginalis and fluorescent Pseudomonas species. Plant Dis. 75:715-720.

Dillon, M. M., Thakur, S., Almeida, R. N. D., Wang, P. W., Weir, B. S., and Guttman, D. S. 2019. Recombination of ecologically and evolutionarily significant loci maintains genetic cohesion in the Pseudomonas syringae species complex. Genome Biol. 20:3.

Excoffier, L., Smouse, P. E., and Quattro, J. M. 1992. Analysis of molecular variance inferred from metric distances among DNA haplotypes: Application to human mitochondrial DNA restriction data. Genetics 131:479-491.

Gardan, L., Shafik, H., Belouin, S., Broch, R., Grimont, F., and Grimont, P. A. D. 1999. DNA relatedness among the pathovars of Pseudomonas syringae and description of Pseudomonas tremae sp. nov. and Pseudomonas cannabina sp. nov. (ex Sutic and Dowson 1959). Int. J. Syst. Evol. Microbiol. 49:469-478.

Gray, F. A., and Hollingsworth, C. R. 2015. Pages 60-62 in: Compendium of Alfalfa Diseases and Pests, 3rd ed. D. A. Samac, L. H. Rhodes, and W. O. Lamp, eds. American Phytopathological Society, St. Paul, MN.

Gross, D. C., and DeVay, J. E. 1977. Role of syringomycin in holcus spot of maize and systemic necrosis of cowpea caused by Pseudomonas syringae. Physiol. Plant Pathol. 11:1-11, IN1-IN2.

Guilbaud, C., Morris, C. E., Barakat, M., Ortet, P., and Berge, O. 2016. Isolation and identification of Pseudomonas syringae facilitated by a PCR targeting the whole P. syringae group. FEMS Microbiol. Ecol. 92:fiv146.

Heydari, A., Kodakaramian, G., and Zafari, D. 2012. Characterization of Pseudomonas viridiflava causing alfalfa root rot disease in Hamedan Province of Iran. J. Plant Pathol. Microb. 3:135.

Hirano, S. S., Clayton, M. K., and Upper, C. D. 1994. Estimation of and temporal changes in means and variances of populations of Pseudomonas syringae on snap bean leaflets. Phytopathology 84:934-940.

Hirano, S. S., Rouse, D. I., and Upper, C. D. 1987. Bacterial ice nucleation as a predictor of bacterial brown spot disease on snap beans. Phytopathology 77:1078-1084.

Huelsenbeck, J. P., and Ronquist, F. 2001. MRBAYES: Bayesian inference of phylogenetic trees. Bioinformatics 17:754-755.

Hwang, M. S. H., Morgan, R. L., Sarkar, S. F., Wang, P. W., and Guttman, D. S. 2005. Phylogenetic characterization of virulence and resistance phenotypes of Pseudomonas syringae. Appl. Environ. Microbiol. 71:5182-5191.

Kamvar, Z. N., Tabima, J. F., and Grünwald, N. J. 2014. Poppr: An R package for genetic analysis of populations with clonal, partially clonal, and/or sexual reproduction. PeerJ 2:e281.

Lamichhane, J. R., Messéan, A., and Morris, C. E. 2015. Insights into epidemiology and control of diseases of annual plants caused by the Pseudomonas syringae species complex. J. Gen. Plant Pathol. 81:331-350.

Lamichhane, J. R., and Venturi, V. 2015. Synergisms between microbial pathogens in plant disease complexes: A growing trend. Front. Plant Sci. 6:385.

Lipps, S. M., Lenz, P., and Samac, D. A. 2019. First report of bacterial stem blight of alfalfa caused by Pseudomonas viridiflava in California and Utah. Plant Dis. 103:3274.

Lipps, S. M., and Samac, D. A. 2022. Pseudomonas viridiflava: An internal outsider of the Pseudomonas syringae species complex. Mol. Plant Pathol. 23:3-15.

Lipps, S. M., Samac, D. A., and Ishii, S. 2022. Genome sequence resource for strains of Pseudomonas syringae Phylogroup 2b and P. viridiflava Phylogroup 7a causing bacterial stem blight of alfalfa. Phytopathology 112: 2028-2031.

Lukezic, F. L., Leath, K. T., and Levine, R. G. 1983. Pseudomonas viridiflava associated with root and crown rot of alfalfa and wilt of birdsfoot trefoil. Plant Dis. 67:808-811.

Misas-Villamil, J. C., Kolodziejek, I., Crabill, E., Kaschani, F., Niessen, S., Shindo, T., Kaiser, M., Alfano, J. R., and van der Hoorn, R. A. L. 2013. Pseudomonas syringae pv. syringae uses proteasome inhibitor syringolin A to colonize from wound infection sites. PLoS Pathog. 9:e1003281.

Morris, C. E., Lacroix, C., Chandeysson, C., Guilbaud, C., Monteil, C., Piry, S., Rochelle-Newall, E., Fiorini, S., Van Gijsegem, F., Barny, M. A., and Berge, O. 2022. Comparative abundance and diversity of populations of the Pseudomonas syringae and soft rot Pectobacteriaceae species complexes throughout the Durance River catchment from its French Alps sources to its delta. bioRxiv 506731.

Morris, C. E., Lamichhane, J. R., Nikolić, I., Stanković, S., and Moury, B. 2019. The overlapping continuum of host range among strains in the Pseudomonas syringae complex. Phytopathol. Res. 1:4.

Morris, C. E., Monteil, C. L., and Berge, O. 2013. The life history of *Pseudomonas syringae*: Linking agriculture to earth system processes. Annu. Rev. Phytopathol. 51:85-104.

Morris, C. E., Sands, D. C., Vinatzer, B. A., Glaux, C., Guilbaud, C., Buffière, A., Yan, S., Dominguez, H., and Thompson, B. M. 2008. The life history of the plant pathogen *Pseudomonas syringae* is linked to the water cycle. ISME J. 2:321-334.

Paynter, V. A., and Alconero, R. 1979. A specific fluorescent antibody for detection of syringomycin in infected peach tree tissues. Phytopathology 69:493-496.

Sackett, W. G. 1910. A bacterial disease of alfalfa. Colo. Agric. Exp. Stn. Bull. 158.

Samad, A., Antonielli, L., Sessitsch, A., Compant, S., and Trognitz, F. 2017 Comparative genome analysis of the vineyard weed endophyte *Pseudomonas viridiflava* CDRTc14 showing selective herbicidal activity. Sci. Rep. 7: 17336.

Sarkar, S. F., and Guttman, D. S. 2004. Evolution of the core genome of *Pseudomonas syringae*, a highly clonal, endemic plant pathogen. Appl. Environ. Microbiol. 70:1999-2012.

Sorensen, K. N., Kim, K.-H., and Takemoto, J. Y. 1998. PCR detection of cyclic lipodepsinonapeptide-producing *Pseudomonas syringae* pv. *syringae* and similarity of strains. Appl. Environ. Microbiol. 64:226-230.

Xin, X.-F., Kvitko, B., and He, S. Y. 2018. *Pseudomonas syringae*: What it takes to be a pathogen. Nat. Rev. Microbiol. 16:316-328.

Zheng, X.-Y., Spivey, N. W., Zeng, W., Liu, P.-P., Fu, Z. Q., Klessig, D. F., He, S. Y., and Dong, X. 2012. Coronatine promotes *Pseudomonas syringae* virulence in plants by activating a signaling cascade that inhibits salicylic acid accumulation. Cell Host Microbe 11:587-596.